Single particle measurements of the chemical composition of cirrus ice residue during CRYSTAL-FACE

D. J. Cziczo,[1,2] D. M. Murphy,[1] P. K. Hudson,[1,2] and D. S. Thomson[1,2]

Received 31 July 2003; revised 10 November 2003; accepted 24 December 2003; published 18 February 2004.

[1] The first real-time, in situ, investigation of the chemical composition of the residue of cirrus ice crystals was performed during July 2002. This study was undertaken on a NASA WB-57F high-altitude research aircraft as part of CRYSTAL-FACE, a field campaign which sought to further our understanding of the relation of clouds, water vapor, and climate by characterizing, among other parameters, anvil cirrus formed about the Florida peninsula. A counter flow virtual impactor (CVI) was used to separate cirrus ice from the unactivated interstitial aerosol particles and evaporate condensed-phase water. Residual material, on a crystal-by-crystal basis, was subsequently analyzed using the NOAA Aeronomy Laboratory's Particle Analysis by Laser Mass Spectrometry (PALMS) instrument. Sampling was performed from 5 to 15 km altitude and from 12° to 28° north latitude within cirrus originating over land and ocean. Chemical composition measurements provided several important results. Sea salt was often incorporated into cirrus, consistent with homogeneous ice formation by aerosol particles from the marine boundary layer. Size measurements showed that large particles preferentially froze over smaller ones. Meteoritic material was found within ice crystals, indicative of a relation between stratospheric aerosol particles and tropospheric clouds. Mineral dust was the dominant residue observed in clouds formed during a dust transport event from the Sahara, consistent with a heterogeneous freezing mechanism. These results show that chemical composition and size are important determinants of which aerosol particles form cirrus ice crystals. *INDEX TERMS:* 0305 Atmospheric Composition and Structure: Aerosols and particles (0345, 4801); 0320 Atmospheric Composition and Structure: Cloud physics and chemistry; 0365 Atmospheric Composition and Structure: Troposphere—composition and chemistry; 1610 Global Change: Atmosphere (0315, 0325); *KEYWORDS:* cirrus ice, single particle, chemical composition

Citation: Cziczo, D. J., D. M. Murphy, P. K. Hudson, and D. S. Thomson (2004), Single particle measurements of the chemical composition of cirrus ice residue during CRYSTAL-FACE, *J. Geophys. Res.*, *109*, D04201, doi:10.1029/2003JD004032.

1. Introduction

[2] Cirrus clouds are an important factor in Earth's climate. Despite minimal physical and optical thickness and ice crystal concentration, when compared to other tropospheric clouds, they can exert a large radiative forcing owing to their extensive global coverage and high altitude [*Liou*, 1986; *Hartmann et al.*, 1992; *Intergovernmental Panel on Climate Change* (*IPCC*), 2001]. The existence of cirrus near the tropopause can reduce the outgoing longwave flux by several W m^{-2} and cause significant radiative heating in this region of the atmosphere [*Jensen et al.*, 1999]. Previous studies have sought to understand the formation, persistence, and habit of these high-altitude clouds [*Heymsfield and Miloshevich*, 1995], but little is known about the chemical composition of the aerosol particles responsible for the formation of the ice crystals which compose cirrus. Without such information it remains uncertain if anthropogenic activities have had a significant impact on this aspect of global climate [*IPCC*, 2001].

[3] Whereas cirrus in the midlatitudes are, in general, generated by synoptic-scale uplift, those formed in the tropics are often the result of convective systems. These clouds are referred to as anvil, or tropical, cirrus because they result from windshear-induced blowoff from the tops of convective anvils as they reach, and often penetrate, the tropopause [*Knollenberg et al.*, 1982]. Few measurements of anvil cirrus microphysical properties have been made owing to their high altitude and often remote locations. *Heymsfield and McFarquhar* [1996] compared observations from mid-1970s WB-57F aircraft measurements from Kwajalein in the Marshall Islands and the mid-1990s Central Equatorial Pacific Experiment (CEPEX). They report the effective particle diameter of ice crystals, d_e, which dropped from 440 to 60 μm, and the ice water content (IWC) from 0.1 to 0.004 g m^{-3} with decreasing cloud temperature from −20° to −70°C. Ice crystals less than ∼100 μm diameter were found to contribute more than half the mass at temperatures below −50°C. Crystal habit was also observed to

[1] Aeronomy Laboratory, National Oceanic and Atmospheric Administration, Boulder, Colorado, USA.
[2] Also at Cooperative Institute for Research in Environmental Sciences, University of Colorado, Boulder, Colorado, USA.

0148-0227/04/2003JD004032$09.00

depend on temperature, with columns replacing bullet-rosettes, hexagonal plates, and nonspherical particles at the lower temperatures.

[4] The dearth of information available on tropical cirrus and their interrelation with atmospheric water vapor and global climate was cited as the motivation for a detailed study using six research aircraft in coordination with ground stations, satellite overflights, and model studies [*Jensen et al.*, 2004]. This field campaign occurred during July 2002 and investigated cirrus formed from intense daily summertime convection, predominately in the Florida region. Two additional flights were made as far south as 12° north latitude. A principal mission objective was to characterize the background aerosol and the subset of particles on which cirrus ice crystals formed.

[5] Historically, two methods have been used to determine the composition of aerosol particles which act as precursors to atmospheric ice crystals. First, collections of cirrus and contrail ice have been made [*Heintzenberg et al.*, 1996; *Petzold et al.*, 1998; *Twohy and Gandrud*, 1998]. Condensed-phase water was melted and evaporated, and the residual material was transported to a laboratory for investigation using electron microscope techniques. In general, these studies suggest that crustal and metallic material are enhanced in cirrus ice when compared to their abundance in the atmosphere. These analyses were limited by the loss of volatile and semivolatile condensed-phase aerosol components during sample preparation, extensive laboratory time required for each particle, and artifacts associated with the collection of large atmospheric ice crystals (D. M. Murphy et al., Particle generation and resuspension in aircraft inlets when flying in clouds, submitted to *Aerosol Science Technology*, 2003, hereinafter referred to as Murphy et al., submitted manuscript, 2003). Second, researchers have developed a continuous flow diffusion chamber (CFDC) to mimic the low-temperature and high-saturation conditions that cause the formation of cirrus clouds [*Chen et al.*, 1998]. This instrument has been flown in the upper troposphere to characterize those particles that are capable of forming cirrus ice under specific conditions. Temperatures have been restricted to those above −35°C and relative humidities (RHs) from 80 to 110% with respect to liquid water. This is significant because the spontaneous formation of ice within micrometer-sized aqueous drops, commonly termed homogeneous freezing, does not occur for water or the ubiquitous background upper tropospheric/lower stratospheric (UT/LS) sulfate aerosol particles [*Murphy et al.*, 1998a] until lower temperatures are reached [*Pruppacher and Klett*, 1978; *Cziczo and Abbatt*, 1999; *Chen et al.*, 2000; *Bertram et al.*, 2000; *Prenni et al.*, 2001]. *Chen et al.* [1998] was therefore restricted to observations of ice formation initiated by an insoluble surface, termed heterogeneous freezing. *Chen et al.* [1998] showed an ice residue mode size of ∼0.2 μm diameter with a few larger than ∼1.0 μm. Chemical composition was determined using traditional electron microscope techniques. As with the aforementioned collection studies, a high frequency of crustal and metallic material was observed although volatile, and semivolatile components were not resolvable.

[6] Here we present measurements of the chemical composition of cirrus ice residue on a single particle basis. The NOAA Aeronomy Laboratory's PALMS instrument was coupled to a CVI in order to characterize the residue of UT/LS ice crystals. The apparatus was flown as part of the scientific payload aboard a NASA WB-57F during CRYSTAL-FACE. We describe ice residue analyzed in cirrus encountered over land and ocean from the Florida area to the Yucatan peninsula, as well as clouds formed during a mineral dust transport event from Africa. We compare the chemical composition of the cirrus ice residue with unactivated aerosol particles (those within clouds that did not nucleate ice) and particles outside cirrus. This is the first report of real time, in situ, measurements of the chemical composition of the particles which cause cirrus ice formation.

2. Experiment

2.1. PALMS

[7] The PALMS instrument has been described in detail previously [*Thomson et al.*, 2000]. Modifications were made to better analyze cirrus ice residue. Aerosol particles are now acquired through an isobaric aerodynamic focusing inlet held at 43 ± 5 torr [*Schreiner et al.*, 2002]. A series of seven orifices, decreasing in size from 0.14 to 0.05 cm diameter, are used to focus particles. Transmission studies were performed using polystyrene latex (PSL) spheres from 0.2 to 1.0 μm diameter and of a known number density. A roughly constant transmission plus analysis efficiency of 0.002 (i.e., two particles were transmitted to the instrument and analyzed per thousand entering the inlet) was observed. Because PALMS produces a high signal-to-noise mass spectrum from >90% of detected particles, regardless of size, the transmission efficiency of the aerodynamic inlet alone is essentially the same as this value and does not appear to have a size bias. Particle sizes reported here range slightly beyond the calibrated range, from ∼0.1 to ∼1.5 micrometers diameter.

[8] Beyond the inlet, two continuous 532 nm Nd:YAG laser beams are used to detect and size atmospheric particles. The beam configuration is shown in Figure 1. Ideally, aerosol particles pass first through the timing beam at which point a clock is started. Time is measured until particles traverse the known distance to the detection beam. The particle aerodynamic diameter, d_{pa}, can be calculated according to *Wilson and Liu* [1980]:

$$d_{pa}^2 = (9\ \mathrm{Stk}\ \mu\ W)/g(C_c\,\rho_p\,v_g), \quad (1)$$

where μ is the temperature-dependent air viscosity, W is the diameter of the final focusing inlet orifice, ρ_p is the particle density (defined here as unity when calculating aerodynamic diameter), v_g is the gas velocity (sonic for this inlet), and the dimensionless Stoke's Number, Stk, is a function of the observed particle transit velocity divided by the gas velocity. Because the slip correction, C_c, is an empirically determined function of the aerodynamic diameter and pressure, d_{pa} is iteratively determined. The low inlet pressure results in a slip correction that is almost proportional to the physical diameter of the particle. Hence the functional dependence is somewhat different than would be found at atmospheric pressure. Aerodynamic sizes presented here were calibrated using equation (1) and PSL spheres from 0.2 to 1.0 micrometers diameter, resulting in

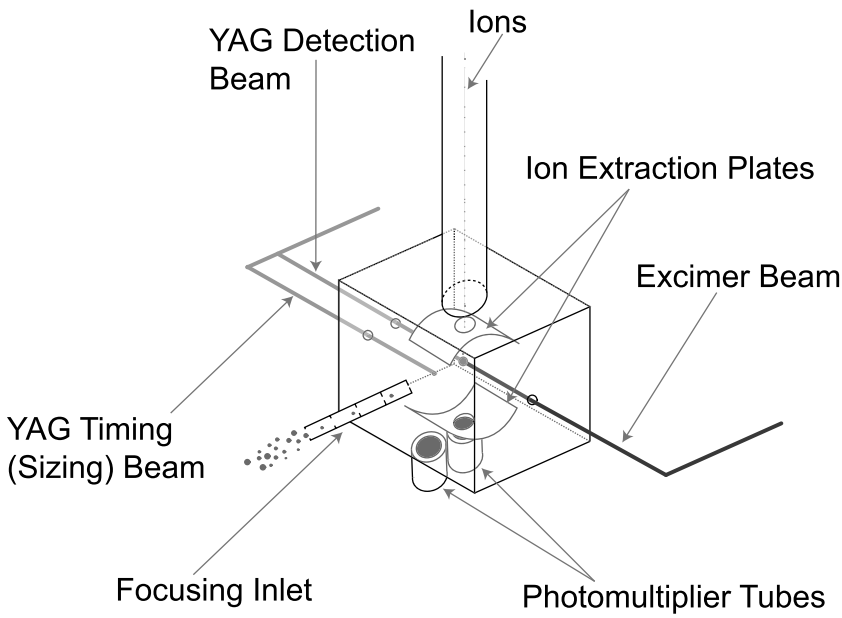

Figure 1. View of the PALMS source region. Dual Nd:YAG laser beams, set 33.14 mm apart, are used to determine particle velocity after exit from the aerodynamic focusing inlet. All particles passed through the second (detection) beam so that an excimer laser could be triggered to strike each aerosol. Nd:YAG laser alignment during CRYSTAL-FACE resulted in ~20% of particles passing through the first (timing) beam as well. Voltage applied to two plates extracts either positive or negative ions which then pass to a TOF reflectron. A high signal-to-noise mass spectrum is produced from >90% of detected particles. Approximately 55% of the CRYSTAL-FACE sample time was spent in positive ion mode with the remainder in negative polarity.

an uncertainty less than ±0.05 micrometers. Laser beam alignment restricted sizing information to ~20% of particles analyzed during CRYSTAL-FACE. The remainder traversed only the detection beam. Scattering from this beam is used to trigger a 193 nm excimer laser with the magnitude of scattered light providing a secondary measurement of size when it is assumed that particles pass through the center, and not the edge, of the detection beam. *Murphy et al.* [2004] have shown that when chemical composition is used to assign realistic particle densities and refractive indices, excellent agreement is found between the aerodynamic and optical particle sizes. Upon striking a particle, the excimer beam vaporizes and ionizes aerosol particle components. Ions are accelerated down a time-of-flight (TOF) reflectron mass spectrometer and impact a microchannel plate detector. A high signal-to-noise positive or negative mass spectrum is thus produced for each aerosol particle analyzed, with >90% of the particles which traverse the detection beam yielding mass spectra. Small aerosol particles, those under ~0.2 μm diameter, are detected with lower efficiency because insufficient scattered light from the detection beam is produced to trigger the excimer laser. No particles <0.12 μm diameter were observed during CRYSTAL-FACE, and this constitutes the lower instrument threshold. The upper threshold of particles larger than ~2.0 micrometers diameter is set by a combination of low atmospheric number density and inefficient transmission through the inlet and instrument.

2.2. CVI

[9] One challenge in sampling the aerosol particles upon which cirrus ice forms is finding a way to collect large ice crystals tens of micrometers in diameter. Furthermore, most of the aerosol particle number density within clouds remains in the form of submicrometer unactivated, or interstitial, aerosol particles. These unfrozen particles must be excluded with high probability in order to maintain data quality.

[10] Cloud particles, both aqueous and frozen, have historically been separated from the interstitial aerosol using counter flow virtual impaction [*Ogren et al.*, 1985]. The operational principle is to direct a counter flow against the motion of the aircraft. Unactivated particles entering the CVI, initially with a relative velocity equal to the air speed, have insufficient inertia to penetrate the counter flow to a region where the flow field becomes zero, known as the stagnation plane. Cloud drops or ice crystals with the same velocity but greater inertia are able to penetrate the stagnation region and enter a sample flow directed toward analytical instruments beyond. The rate of counter flow, coupled with the air speed and ambient conditions, defines the cutpoint of particles subject to experimentation.

[11] The CVI used during these studies, shown schematically in Figure 2, is based on the design of *Laucks and Twohy* [1998]. There are four principal differences between the designs. First, this CVI is vacuum-jacketed in order to minimize thermal gradients. Second, the inner diameter is stepped from 4.0 to 7.0 mm instead of a ~6.0 mm tip diameter in order to maximize ice crystal residence time in the dry heated section of the CVI. Third, a 1.2 cm cylinder of porous stainless steel frit (GKN Sinter Metals), instead of 8.0 cm, was used to introduce the counter flow. The fourth principal difference between this and the design of Laucks and Twohy is that the sample flow to PALMS was drawn from 90° off the CVI flow path so that large particles were

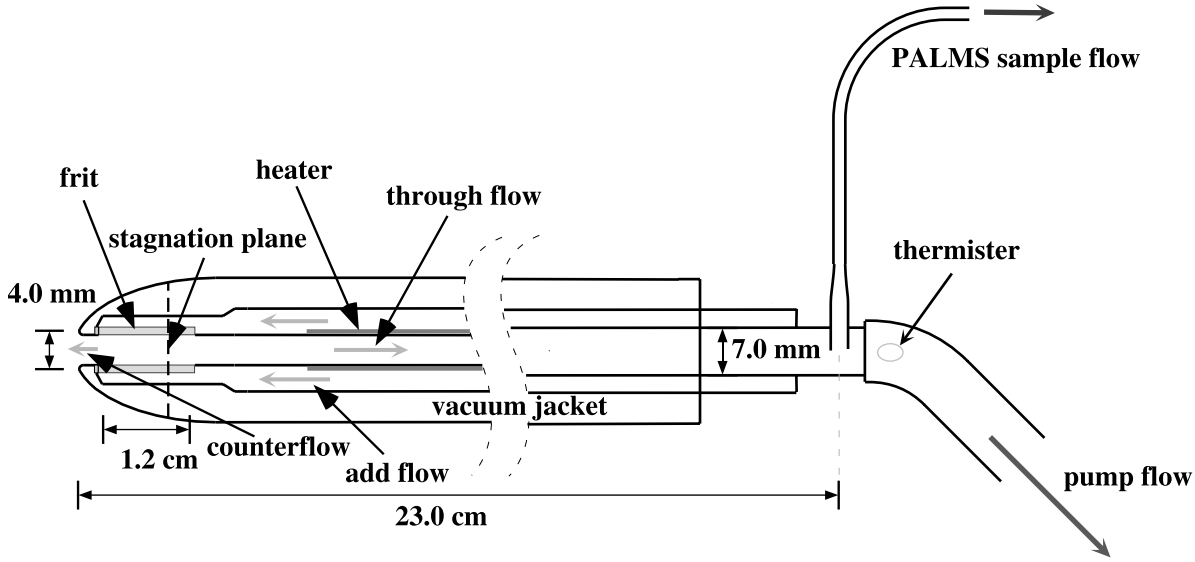

Figure 2. Schematic diagram of the counter flow virtual impactor used during CRYSTAL-FACE. The add flow-passed through a porous stainless steel frit separated into a counter flow used to exclude small particles and a through flow directed toward PALMS. The relative rates of the two flows determined a stagnation plane where the flow velocity was nearly zero. During CRYSTAL-FACE, an add flow of 4.0 lpm, a counter flow of 3.0 lpm, and a through flow of 1.0 lpm were used, resulting in a stagnation plane approximately 0.9 cm from the forward end of the frit. The through flow, subsequently heated to melt and evaporate ice crystals, was split into a 0.9 lpm sample flow to the PALMS instrument 23.0 cm from the inlet and a 0.1 lpm flow directed to a pump where temperature was measured using a thermister. Using these values, a lower ice crystal cutpoint of approximately 5 μm and an upper cutpoint of 22 μm can be estimated (see text for details). Interstitial aerosol and particles outside clouds were sampled by reducing the add flow to 0.1 lpm, increasing the through flow to 4.5 lpm, and maintaining the PALMS sample flow. In this case all particles, regardless of size, were admitted through the CVI.

excluded from analysis. The lower particle cutpoint can be estimated by comparing the location of the stagnation plane relative to the inlet tip to the particle stopping distance, S, given approximately by *Willeke and Baron* [1992]:

$$S = \left(v_0 \rho_p d_p^2 C_c\right)/(18\ \mu), \tag{2}$$

where v_0 is the initial particle velocity, in this case equivalent to the air speed; ρ_p is the particle density, in this case assumed to be that of water ice; and d_p is the particle diameter, assumed to be spherical. Using reasonable values for air speed (150–200 m/s) and pressure (12–15 km altitude), the cutpoint diameter for particles able to penetrate the stagnation plane described in Figure 2 is approximately 5 μm. Cirrus ice larger than this size entered a low water vapor flow (dewpoint less than −40°C) heated from ambient to −10°C for 400 ms within the CVI and then to 10°C during the 50 ms transit time between the CVI and PALMS analysis. Crystals were evaporated in this manner, leaving ice residue roughly the size of the aerosol particles on which the ice initially formed (see section 2.3). Large ice crystals with a stopping distance in excess of the 23 cm length of this region would have penetrated the length of the CVI without a significant reduction in velocity. This velocity reduction step, from aircraft speed to flow velocity, 0.4 m/s, is critical in that large ice crystals would not reside within the CVI for sufficient time to evaporate or melt. These particles would have either been pumped away or impacted the aft wall of the CVI. Using equation (2), this corresponds to crystals larger than ∼22 micrometers in diameter.

[12] Of considerable interest during CRYSTAL-FACE was comparison of ice residue to both those particles that did not nucleate ice within clouds and to those outside cirrus. In order to analyze these predominantly submicrometer particles, the counter flow was reduced to zero while maintaining the sample flow to PALMS. Under these conditions, all particles, regardless of size, passed through the CVI. Outside cirrus the background aerosol was sampled 80% of the flight time, whereas within cloud the interstitial aerosol was sampled 30% of the time. The data presented here are therefore grouped into the categories of "ice residue," "interstitial aerosol," and "outside cloud." See Appendix A for further details.

2.3. Limitations and Uncertainties

[13] There are several noteworthy limitations of the technique described here for the determination of the chemical composition of cirrus ice residue. Except in the case of compositionally simple systems that can be studied in the laboratory [*Thomson et al.*, 1997; *Cziczo et al.*, 2001], mass spectra acquired by single particle instruments such as PALMS are qualitative data. Substances commonly found in atmospheric aerosol particles can ionize with considerably different efficiencies. The particle matrix also affects the ablation and ionization processes so that an identical abundance of a specific material may create variable

signals in different aerosol types (e.g., 1 wt% iron dissolved in sulfuric acid as opposed to incorporated as a crystalline solid into mineral dust). Comparisons of instruments colocated at the same field site has shown, even if the data are not fully quantitative, that PALMS and similar instruments are capable of showing trends in chemical composition [*Middlebrook et al.*, 2003; *Gross et al.*, 2000]. The data presented here should be viewed in this context, not as quantitative data.

[14] Although counter flow virtual impaction is a powerful tool for the separation of cloud elements from interstitial aerosol, it does introduce three limitations to this data set. First, during CRYSTAL-FACE, roughly 90% of the mass spectra acquired within cirrus with the counter flow on were consistent with submicrometer stainless steel particles, identified by the presence of iron, chromium, and molybdenum. Ice crystals sampled by high-speed research aircraft have sufficient inertia to impact the walls of traditional inlets and counter flow virtual impactors. The impaction process can result in the liberation of material from inlet surfaces, as well as previously deposited material. This has had an undetermined effect on previous aircraft studies within liquid and ice clouds. Laboratory studies have shown that the frit and tubing used during CRYSTAL-FACE is susceptible to the impaction process (Murphy et al., submitted manuscript, 2003). Analysis of ice residue on a crystal-by-crystal basis allowed for the removal of all mass spectra with features similar to stainless steel from this data set. This was done to ensure quality but also means that any metallic ice nuclei (IN) have been eliminated from this data set. This is significant because many metal IN may be of anthropogenic origin [*DeMott et al.*, 2003a], but this information is lost from this study. Second, as described in the previous section and in Appendix A, the CVI used in these studies efficiently sampled the residue of ice crystals 5–22 μm in diameter. The number size distribution of cirrus ice during CRYSTAL-FACE peaked at ~30 μm diameter with large crystals up to 1000 micrometers commonly observed (D. Baumgardner, Universidad Nacional Autónoma de México, personal communication, 2003). The largest crystals likely form first within a convective system, at the lowest saturation and highest temperature conditions, owing to heterogeneous nucleation of the most effective IN [*DeMott et al.*, 1997]. The restriction of these data to ice residue from crystals just smaller than average likely adds bias to ice formed higher and later in the convection process (i.e., at higher saturations and lower temperature). Third, the process of separation and heating subjected small ice crystals to a residence time equal to the CVI volume divided by the flow rate, or ~0.4 s. The loss of highly volatile species, besides water, by evaporation at these timescales is unknown.

[15] Cloud structure and density imposed three important limits on data acquisition. First, anvil cirrus are formed from intense convective cells which are spatially much smaller than the resulting high-altitude cloud. Large ice is subject to higher fall velocities than small crystals. These factors lead to cloud heterogeneity such that the course flown by the investigating aircraft affects sample properties. The effect that cloud structure has on these data is unknown. Second, after formation, cirrus ice crystals can effectively scavenge both gas-phase species and particles [*Abbatt*, 2003; *Vohl et al.*, 2001], thus changing the chemical composition of the ice residue from the particle on which ice formed. Previous collections of cirrus and contrail ice do not indicate a high frequency of multiple IN per crystal [*Heintzenberg et al.*, 1996; *Petzold et al.*, 1998; *Twohy and Gandrud*, 1998]. On the basis of observations of ice residue versus interstitial aerosol particle size in cirrus during the 2000 Interhemispheric Differences in Cirrus Properties From Anthropogenic Emissions (INCA) experiment, *Seifert et al.* [2002] suggest the fraction of crystals that have scavenged an interstitial aerosol particle is insignificant (<1%). This topic is discussed in more detail in section 4. Third, the low number density of ice crystals (typically <1% that of the background aerosol) and the short periods of time during which the aircraft was within cloud contributed to a low total number of ice residue sampled (~1750 after elimination of artifacts). Whereas particle mass spectrometers normally analyze the composition of background aerosol particles at several Hz for long time periods [*Middlebrook et al.*, 2003] the aforementioned limitations preclude this sampling rate or duration. This study describes the composition of similar or greater numbers of ice residue than in previous works [*Heintzenberg et al.*, 1996; *Petzold et al.*, 1998; *Twohy and Gandrud*, 1998; *Chen et al.*, 1998], but results should be placed within this statistical perspective.

3. Results and Discussion

[16] The NASA WB-57F that participated in the CRYSTAL-FACE mission made a total of 12 cirrus measurement flights from Key West Naval Air Station during the month of July 2002 [*Jensen et al.*, 2004]. Two of these, hereinafter referred to as the southern flights, were south through the Yucatan Channel and along the Central American coast to approximately 12° north latitude (the 9th and 26th). Two more (the 28th and 29th), the dust event flights, were made along the Florida Gulf Coast during the peak of an intense mineral dust transport event from the Sahara Desert [*Sassen et al.*, 2003; *DeMott et al.*, 2003b]. The remainder (the 3rd, 7th, 11th, 13th, 16th, 19th, 21st, and 23rd), the Florida area flights, were made near or over the Florida Peninsula.

[17] More than 14,400 high signal-to-noise mass spectra of individual aerosol particles, after subtraction of stainless steel inlet artifacts, were acquired during the flights. Particles encountered in the UT/LS outside the confines of cirrus clouds, hereinafter referred to as the ''outside cloud,'' represented 71% of the total, with roughly equivalent numbers analyzed in positive and negative ion mode. ''Interstitial aerosol'' represented 17% of the total, with 57% of these particles in positive and 43% in negative ion mode. Less than 5% of these were eliminated when cloud ice crystal density was large (see Appendix A). The remaining 12% of particles were sampled as cirrus ''ice residue,'' 53% in positive and 47% in negative ion mode. There were flight-to-flight differences in particle number analyzed owing to density variations, flight time, time in cloud, and instrument performance.

[18] Aerodynamic diameter was determined for approximately one in five analyzed particles (see section 2.1). As with the total number of particles analyzed, instrument performance (i.e., laser beam alignment) differed between flights and resulted in disparate determination rates. Size

distributions, separated by collection method and flight during which analysis occurred, are shown in Figure 3. Figure 3a, for example, is a histogram of size for those particles analyzed outside cloud. The principal mode size is 0.4 micrometers diameter tailing to the lower instrument threshold at 0.12 μm. Figure 3c illustrates the presence of two modes for the interstitial aerosol particles sampled during CRYSTAL-FACE: a more populous mode also at 0.4 and a larger mode 0.7 μm diameter. These, and size distributions for ice residue, are described in the next three sections.

[19] In order to facilitate data analysis, mass spectra were categorized by hierarchical cluster analysis [*Murphy et al.*, 2003] into 30 positive and 20 negative particle categories. The positive categories were further combined into four general groups: those with dominant spectral features owing to sulfate species, K^+, organic fragments, and NO^+ (abbreviated SKON, 88%), sea salt (4%), refractory materials attributed to mineral dust and fly ash (7%), and all other species (1% total and no more than 2% of the spectra analyzed on any single flight). Sulfates, organics, and NO^+ are ubiquitous components of UT/LS aerosol particles [*Murphy et al.*, 1998a]. Potassium is a marker of biomass burning, which had a substantial impact on the aerosol during CRYSTAL-FACE owing to forest fires in the United States and Canada (H.-J. Jost, NASA Ames, personal communication, 2003). These four species were commonly internally mixed in particles such that a continuum of compositions existed, represented by seven of the original categories. The SKON group dominated the particles analyzed both outside cloud (>95%, Figure 3b) and interstitial aerosol (88%, Figure 3d). Particles of this type spanned the observable size range but were predominantly found in the 0.4 μm mode. Sea salt particles have been previously observed in marine locations with the PALMS instrument [*Murphy et al.*, 1998b], but they exist with very low frequency in the UT/LS (<1%). Their numbers were slightly enhanced in the interstitial aerosol (5%). Marine particles were, in general, physically larger than the SKON group, and they form part of a bigger size mode observed for the interstitial aerosol. They are spectroscopically distinct and formed only a single original category. The third group was combined from eight categories, after stainless steel particles were removed, which contained signal from refractory species such as aluminum, silicon, iron, magnesium, calcium, potassium, and sodium. These species are common components of both mineral dust and fly ash, particle types which would produce undifferentiable PALMS mass spectra. As with sea salt, mineral dust or fly ash was uncommon in the cloud-free UT/LS (1%) but slightly enhanced in the interstitial aerosol (6%). Mineral dust and fly ash particles were also larger, in general, than the SKON group and therefore formed part of the large size mode apparent in the interstitial aerosol distribution. In the case of both interstitial sea salt and mineral dust particles, it is probable that convection played a role in the enhancement observed when compared to outside cloud particles by efficient pumping of boundary layer material to high altitude within clouds. This conclusion is tempered by the uncertainty related to sampling small cirrus ice concurrently with interstitial aerosol (see Appendix A) and the low numbers of particles analyzed. The final group, encompassing particles that did not fit into the three previous groups such as vanadium-containing particles attributed to oil combustion, is termed "other."

3.1. Southern Flights

[20] The first southern flight represented a unique opportunity during CRYSTAL-FACE. A geographically large cirrus cloud attributed to convective system blowoff was encountered off the Central American coast [*Jensen et al.*, 2003]. It existed within 1 km of the tropopause and spanned several degrees of latitude centered around 15° north. This was a singular opportunity in that interstitial aerosol and ice residue were analyzed at the same altitude within the same cloud in both positive and negative ion mode. Particles were also analyzed in both polarities just before entering and just after leaving the cloud. At no other time during CRYSTAL-FACE was a single cirrus physically extensive enough to allow for particle analysis in all modes of instrument operation.

[21] The size distributions and chemical compositions of the outside cloud and interstitial aerosol did not differ significantly from the whole mission data (Figures 3a–3d),

Figure 3. (a) Aerodynamic diameter of particles encountered outside cloud from 5.0 to 15.0 km altitude during CRYSTAL-FACE and (b) the distribution of chemical composition of those particles analyzed in positive ion mode. The number of particles incorporated into each histogram is shown in parenthesis. Chemical composition is separated into four groups (see text for details): sulfates, K^+, organics, and NO^+ (SKON, red), sea salt (orange), mineral dust or fly ash (green), and other species (blue). Free tropospheric particles analyzed by PALMS had a dominant size mode of 0.4 micrometers and the vast majority (>95%) were classified in the SKON group. Subsequent panels show (c and d) analogous size distribution and chemical composition information for interstitial aerosol, ice residue collected during (e and f) the southern flights, (g and h) in the Florida area, and during (I and j) the dust event, respectively. Note the interstitial aerosol analyzed during CRYSTAL-FACE had a principal size mode similar to particles outside cloud but with the addition of a larger secondary mode. The chemical composition was also dominated by the first group. Sea salt and mineral dust or fly ash was predominantly found in the large mode, probably lofted from the boundary layer by the convective systems which produced the anvil cirrus clouds under investigation. Ice residue analyzed during the southern flights had two roughly equivalent size modes. Chemical composition in both modes was dominated by the SKON group, consistent with a homogeneous freezing mechanism. The large size mode was predominantly particles tropospheric in composition (see text for details). Ice residue analyzed during flights in the Florida area was dominated by large particles with a composition consistent with sea salt (26%) and mineral dust or fly ash (44%). The frequency with which ice residue was classified as mineral dust or fly ash rose to 64% during the dust event, consistent with freezing occurring principally by a heterogeneous mechanism. The altitude at which data collection occurred is indicated in each aerodynamic diameter panel.

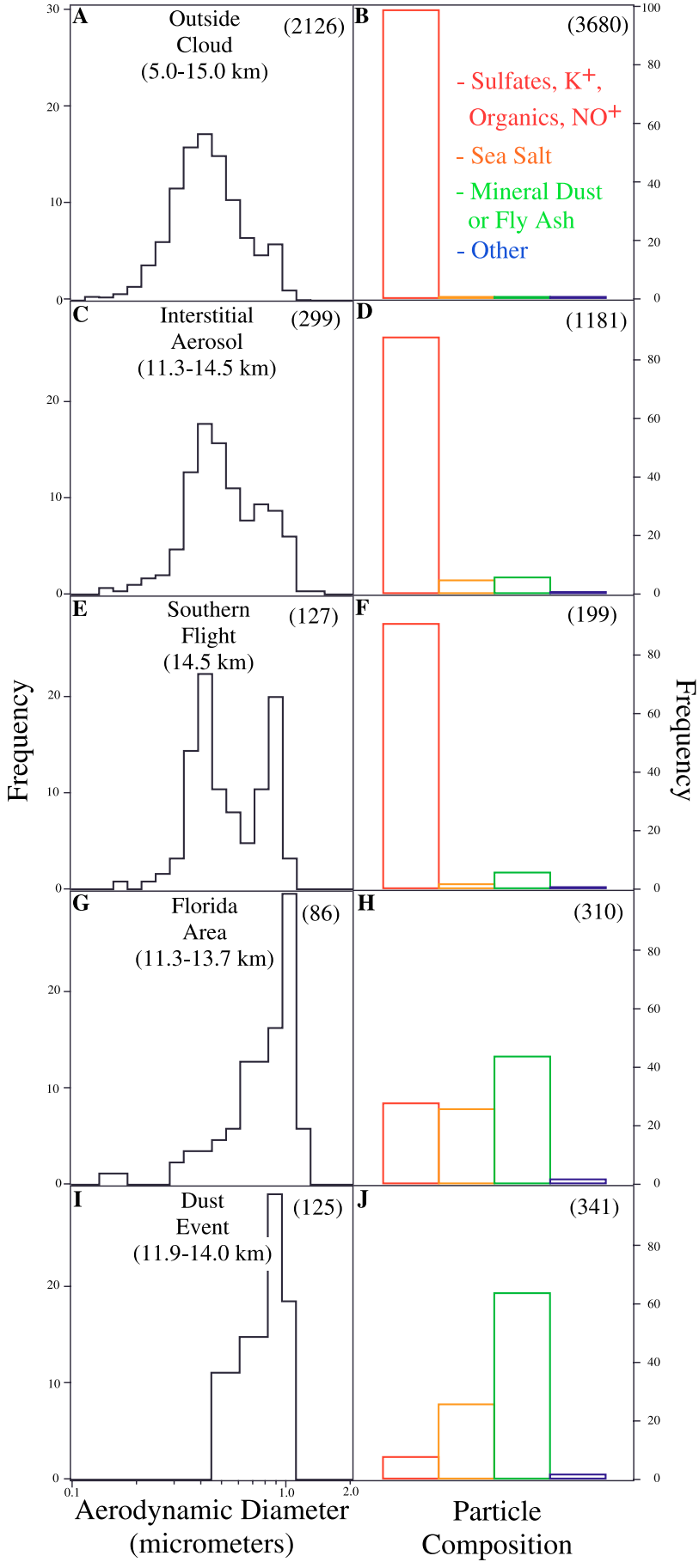
A
Outside
Cloud
(5.0-15.0 km)
(2126)
B
(3680)
- Sulfates, K+,
Organics, NO+
- Sea Salt
- Mineral Dust
or Fly Ash
- Other
C
Interstitial
Aerosol
(11.3-14.5 km)
(299)
D
(1181)
E
Southern
Flight
(14.5 km)
(127)
F
(199)
G
Florida
Area
(11.3-13.7 km)
(86)
H
(310)
I
Dust
Event
(11.9-14.0 km)
(125)
J
(341)
Frequency
Frequency
0.1
1.0
2.0
Aerodynamic Diameter
(micrometers)
Particle
Composition

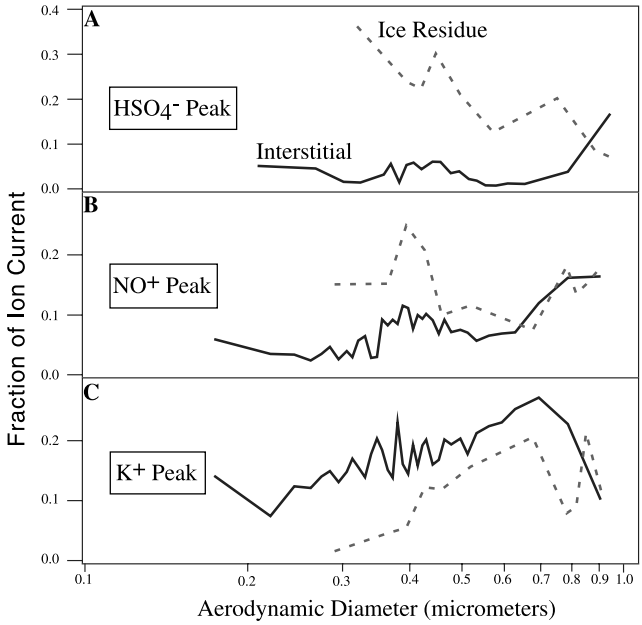

Figure 4. Fraction of detector signal attributed to the HSO_4^- peak, the principal negative polarity fragment of sulfuric acid, as a function of particle size. Data in Figure 4a is plotted for both interstitial aerosol (solid line) and ice residue (dashed line) analyzed during the 9 July 2002 southern flight. Note that small ice residue contained relatively more sulfate than either small interstitial particles or larger ice residue, implying preferential freezing of particles had taken place. Large ice residue and interstitial aerosol appear to be similar. The ion current from the NO^+ peak, owing to species such as ammonium and nitric acid (see text for details), is shown in Figure 4b. An enhancement is present for the smallest ice residue: this concept is expanded in section 4. Similar traces for K^+, a marker of biomass burning, indicate this species is preferentially partitioned to the interstitial aerosol for all but the largest particles observed (Figure 4c). About 500 interstitial aerosol particles and 400 ice residue were analyzed during the southern flight with approximately equal fractions in positive and negative ion mode. The size distributions of interstitial aerosol and ice residue, shown in Figures 3c and 3e, reflect the relative numbers of particles incorporated into Figures 4a–4c.

although particles analyzed outside cloud contained species such as Br, I, and Hg, which have been observed at the tropopause during previous aircraft missions [*Murphy and Thomson*, 2000]. A histogram of the aerodynamic diameter of the ice residue within the cloud is shown in Figure 3e and the chemical composition in Figure 3f. The ice residue is dominated by sulfate, K^+, organic, and NO^+ particles (91%) but, unlike the outside cloud and interstitial aerosol data, two roughly equivalent size modes, 0.4 and 0.9 μm diameter, were present. Very small enhancements in large sea salt (2%) and mineral dust or fly ash (6%) particles, when compared to the UT/LS aerosol particles, do not fully explain the quantity of particles in the larger mode. Ice residue did not contain the species Br, I, or Hg, which is consistent with particles lofted by convection from a lower region of the troposphere. Inclusions of refractory components were not frequently observed in the ice residue, and heterogeneous freezing formation was therefore not likely.

[22] The enhancement of large particles in this ice residue size distribution is most likely a result of the preferentially freezing of large particles over smaller ones. Cloud properties, such as temperature, updraft velocity, and relative humidity, dictate hygroscopic growth and result in a size with maximum dilution and minimum bulk freezing point [*Lin et al.*, 2002; *Pruppacher and Klett*, 1978]. Both classical volumetric [*Pruppacher and Klett*, 1978] and surface area freezing theories [*Tabazadeh et al.*, 2002] suggest nucleation of the ice phase begins for the largest particles. Hygroscopic growth and ice nucleation probability thus combine to favor freezing of the largest and most dilute aqueous particles but only a limited number of physically smaller particles. Given the interstitial aerosol size distribution shown in Figure 3, the ice residue data collected during the southern flights are consistent with freezing of most, if not all, particles greater than approximately 0.75 micrometers diameter (i.e., the less populous but physically larger interstitial aerosol mode). A chemically distinct subset (see next paragraph) of the more populous, but physically smaller, mode was also observed to freeze.

[23] Although the majority of particles outside cloud, interstitial aerosol, and ice residue were grouped as SKON, chemical differences were present between particle types and across the observed size range. Figure 4 shows the detector signal, expressed in fraction of the total current attributed to specific ions owing to three specific species, as a function of particle size and mode in which data was collected. Figure 4a shows the fraction of signal owing to the dominant fragment of sulfuric acid produced in negative polarity, HSO_4^-, for both ice residue and the interstitial aerosol. This sulfate ion is enhanced in the smaller ice residue mode observed in Figure 3e but is similar to the interstitial aerosol for particles larger than ~0.8 μm diameter. This behavior is also shown for the positive NO^+ ion in Figure 4b, with enhancements found for ice residue smaller than ~0.7 micrometers when compared to the interstitial aerosol. Ice residue and interstitial aerosol particles larger than this size exhibit roughly the same signal. As shown in Figure 4c, the biomass burning marker K^+ shows a behavior opposite that of the HSO_4^- and NO^+ ions: greater signal was observed for interstitial aerosol than ice residue smaller than ~0.8 μm. Both particle types had roughly the same signal at larger sizes. These observations are consistent with the argument made in the last paragraph that almost all large particles (>0.75 μm diameter) nucleated ice whereas only a subset of smaller particles, chemically distinct in nature, produced cirrus ice. The low sulfate but high K^+ and organic signal exhibited by the large particles and the interstitial aerosol is consistent with particles observed outside cloud in the lower troposphere. This observation is expanded in section 4.

[24] Previous PALMS flights in the stratosphere have shown that meteoritic material dissolved in sulfuric acid represents ~50% of particles analyzed in positive ion mode but that these aerosol particles are present at very low frequency below the tropopause [*Murphy et al.*, 1998a]. The presence of elements in meteoritic material particles and their ratios are distinct from other metal-containing

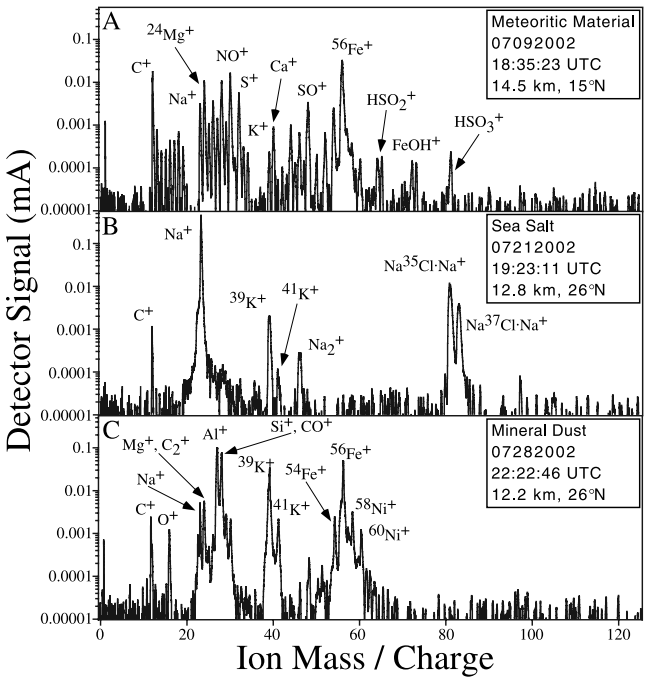

Figure 5. Mass spectra of individual ice crystal residue analyzed in positive ion mode during CRYSTAL-FACE. The detector signal, or ion current, attributed to individual species are labeled in ion mass/charge space. Meteoritic material [*Murphy et al.*, 1998a; *Cziczo et al.*, 2001] was found in cirrus ice crystals encountered within 1 km of the tropopause at 15° north latitude during the southern flights, suggesting the importance of stratospheric aerosols on tropospheric cloud properties (Figure 5a). In the Florida area, sea salt was found within ice crystals with high frequency even though essentially no marine aerosols are found in the free troposphere at this altitude (see Figure 3b), suggesting lofting of considerable boundary layer material by convective systems. Mineral dust was the major ice residue analyzed within cirrus at over 12 km altitude during a dust event (Figure 5c), even though the dust layer was observed at 1–5 km [*Sassen et al.*, 2003]. Note that very little soluble matter, such as sulfates or nitrates, is present on this particle.

particles [*Cziczo et al.*, 2001]. The mass spectrum of the residue of a single ice crystal from the cirrus cloud encountered on the first southern flight is shown in Figure 5a. The elements and the ratios of their signals are identical to previously observed stratospheric meteoritic material. Such spectra represented 4% of the ice residue analyzed in positive ion mode within the cirrus cloud. It is uncertain if stratospheric aerosol particles were entrained in a convective system which overshot the tropopause [*Knollenberg et al.*, 1982], froze, and settled into the troposphere or if a larger-scale circulation was responsible [*Tuck et al.*, 1997]. Meteoritic material aerosol particles are largely sulfuric acid in composition, with small amounts of extraterrestrial metals in solution [*Wise et al.*, 2003]. Insoluble meteoritic components, such as SiO_2 and Al_2O_3, form small inclusions. It remains unknown if these particles entered the ice phase via homogeneous or heterogeneous freezing. Regardless of the mechanism, this is, to our knowledge, the first observation of unambiguously stratospheric aerosol particles forming cirrus ice and demonstrates that such aerosol particles are responsible, in part, for the formation of anvil cirrus.

3.2. Florida Area

[25] The majority of flights made during CRYSTAL-FACE took place over, or along the coasts of, the Florida peninsula. The principal reason for the mission location and season was the intense, almost daily, convection that takes place during summer resulting in tropical cirrus.

[26] The ice residue size distribution for flights in the Florida area is shown in Figure 3g. Unlike particles sampled outside cirrus or the interstitial aerosol, there is no size mode 0.4 micrometers diameter. Instead, the majority of residue was incorporated into a 1.0 μm mode tailing to 0.3 μm. The reason for the large size of the ice residue can be understood by relating it to the chemical composition of the particles which formed ice in the Florida area, shown in Figure 3h. Unlike the composition of either the particles sampled outside cirrus or the interstitial aerosol, the ice residue in the Florida area was not dominated by the SKON group (28%). Instead, 26% of the ice residue was sea salt and 44% mineral dust or fly ash. An example of the residue of a cirrus ice crystal that is marine in origin is shown in Figure 5b. This spectrum is striking in that it is of a recently generated sea salt particle with insignificant chlorine loss or other modification [*Gard et al.*, 1998; *Laskin et al.*, 2002]. This ice residue was analyzed at 12.8 km, where essentially no marine particles (<1%) are found outside cirrus.

[27] The distribution of chemical composition is of interest because it implies that a significant fraction of the ice crystals present in Florida area tropical cirrus, 70%, had an origin as particles incorporated into convective systems at or near the planetary boundary layer since neither sea salt nor mineral dust was present in the free troposphere at significant levels. Sea salt, like sulfates and organics, is believed to enter the ice phase via a homogeneous freezing mechanism whereas mineral dust or fly ash would most likely enter the ice phase heterogeneously. Unlike the southern flights cirrus, clouds observed in the Florida area appeared to incorporate both mechanisms simultaneously. This would be consistent with ice formation initially due to the more efficient (i.e., lower required saturation and temperature) heterogeneous mechanism followed by homogeneous freezing [*DeMott et al.*, 1997].

[28] Also of interest is the high abundance of sea salt found in the ice residue versus a low quantity found in the interstitial aerosol. SKON, conversely, represents the vast majority of interstitial aerosol particles but with lower representation as ice residue. It appears that a mechanism analogous to what was observed during the southern flights was responsible: large, dilute droplets preferentially froze before small ones. During the southern flights, this behavior was exhibited by particles of roughly similar composition. In the Florida area, sea salt appears to have dominated the larger size mode. It is known that NaCl exhibits extensive water uptake, compared to sulfate species such as $(NH_4)_2SO_4$, at a given saturation [*Pruppacher and Klett*, 1978]. Both mechanisms would result in larger, more dilute, sea salt particles and would explain their preferential freezing. It bears noting that no significant differences were observed in ice residue size or

chemical composition for convective systems originating over land versus those formed over water.

3.3. Saharan Dust Event

[29] The meteorology throughout July 2002 resulted in enhanced transport of African mineral dust to the Florida peninsula. A particularly intense event from the Sahara coincided with the last two cirrus measurement flights. A mineral dust layer was observed from 1 to 5 km using both ground-based lidar and airborne instruments. Dust concentrations in Miami exceeded 30 $\mu g\ m^{-3}$ during these days [*Sassen et al.*, 2003]. Backward air trajectories place the origin of this layer in Africa about one week prior to arrival in the Florida area [*DeMott et al.*, 2003b]. The mineral particles were observed to act as efficient, heterogeneous, ice nuclei: *DeMott et al.* [2003b], using an airborne CFDC, showed that IN concentrations within the layer were more than two orders of magnitude greater than the typical median concentration.

[30] The size distribution of the ice residue observed during the dust event is shown in Figure 3i. The peak of the size distribution is 0.9 micrometers diameter, not unlike what was observed on other flights in the Florida area. The chemical composition of ice residue during the dust event was markedly different from all other cirrus measurement flights, however. A minimal amount of the ice residue was classified as SKON (8%). Approximately 25% of ice residue was of marine origin. The majority were consistent with mineral dust or fly ash (64%). Owing to the known presence of a mineral dust layer and the observed ice nucleating efficiency of these particles, it is assumed that these particles were Saharan mineral dust. Unlike the southern flights when freezing proceeded homogeneously through aqueous particles without inclusions, or the Florida area flights where aqueous and refractory particles were roughly equivalently represented in the ice residue, it appears that heterogeneous freezing was responsible for the majority of the cirrus ice observed during the dust event.

[31] A mass spectrum of the residue of a single cirrus ice crystal analyzed during the dust event is shown in Figure 5c. Several refractory materials associated with mineral dust are evident: aluminum, iron, nickel, potassium, and sodium. Noticeably absent are features associated with sulfate and organic fragments or NO^+. Instead, this mass spectrum, typical of the mineral dust particles observed as cirrus ice residue during the dust event, is consistent with a bare refractory surface with a minimal coating of soluble material.

4. Atmospheric Implications

[32] There are several implications of the single particle measurements of the chemical composition of cirrus ice residue during CRYSTAL-FACE described in this work which are important towards gaining a full understanding of the atmosphere. First, the presence of meteoritic material and sea salt as cirrus ice residue provided sources of particles with unambiguous mass spectra. This is important because there is scant field data on the effect of scavenging of gas-phase species or interstitial particles by cirrus ice crystals, and this has hampered attempts to draw conclusions from analyses of ice residue. Unambiguous particle types allowed us to compare mass spectra obtained from ice residue with those outside cloud; the latter assumed to be unaffected by scavenging. A period of the first southern flight is shown in Figure 6. Plotted as a solid line is the concentration of ice crystals observed by the CAPS instrument [*Baumgardner et al.*, 2002] to illustrate the bounds of the cirrus cloud. Circles represent single meteoritic material particles observed outside the cloud whereas squares represent observations within (i.e., ice residue). Figure 6a expresses the signal fraction attributed to sulfate peaks for these meteoritic material particles. The fraction is ~4% for all particles. This result is significant because it implies that minimal scavenging of interstitial particles by crystals or ice coalescence has occurred. The relative sulfate signal would have been perturbed by the addition of other material unless those particles were significantly smaller but devoid of meteoritic material owing to the relative infrequency of this particle type (4%), if particle scavenging had occurred. Figure 6b expresses the fractional signal attributed to the NO^+ peak for the same particles observed during this period. The signal is consistent, ~3%, for the particles outside cloud but significantly higher, 10–25%, for ice residue. The presence of the NO^+ peak has been studied in our lab, and it can be derived from several nitrogen containing species. In this case it seems likely that the cirrus ice within this cloud scavenged gas-phase nitric acid [*Abbatt*, 2003], which then remained on particles through the PALMS analysis process, although we do not have a quantitative understanding of the coverage. Particle-phase scavenging results are generally consistent with the findings of *Seifert et al.* [2002]. We conclude that gas-phase scavenging may have occurred during the southern flights but that scavenging of particles by cirrus ice did not occur frequently and does not significantly alter the data presented here.

[33] The observation of meteoritic material in cirrus ice is significant beyond the conclusion that it provided regarding placing a limit on scavenging. The impact of stratospheric aerosol particles on tropospheric cirrus cloud properties has not been extensively evaluated, but this observation shows that there is a nonnegligible effect in some cirrus. Specifically, 4% of the ice residue analyzed in positive ion mode during the first southern flight was consistent with meteoritic material. Meteoritic material is not obvious in negative ion mode, but there is no reason to assume that the ratio was different. This particle type has been found to represent ~50% of the lower stratospheric aerosol particles in the PALMS size range. We therefore conclude that ~8% of the ice crystals in this cirrus cloud could have originated from stratospheric aerosol. It is intriguing to note that there may be a climatic link between meteoritic material or volcanic eruption and cirrus cloud coverage especially when given the much larger extraterrestrial flux rates and large eruptions that have occurred in the past.

[34] Recent studies have described the formation of ice in the Northern Hemisphere (NH) at Prestwick, Scotland, as predominantly due to heterogeneous freezing on the basis of measurement of temperature, vertical velocity, aerosol particle size, and ice crystal concentration in cirrus clouds from the DLR Falcon research aircraft [*Karcher and Strom*, 2003]. Conversely, measurements from the same platform in the Southern Hemisphere (SH) at Punta Arenas, Chile, suggested

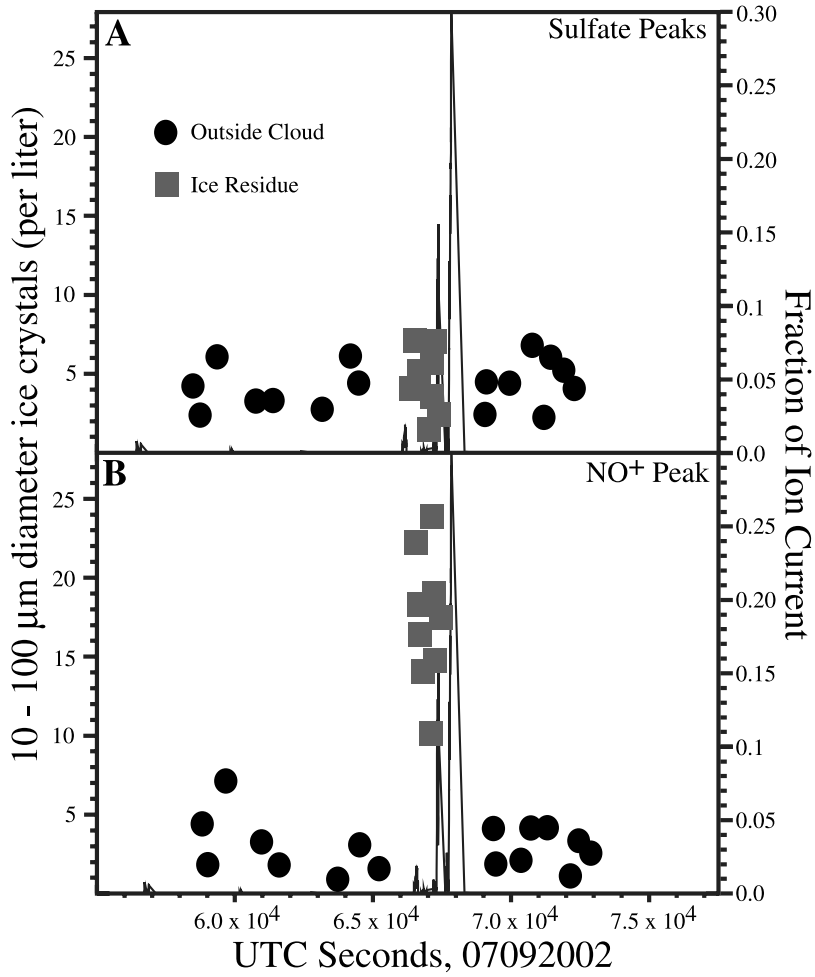

Figure 6. Chemistry of meteoritic particles during a cloudy segment of the 9 July 2002 southern flight. The number density of ice crystals from 10 to 100 micrometers diameter is plotted (solid line) to differentiate particles analyzed as cirrus ice residue (squares) from outside cloud aerosol (circles). Figure 6a shows the fraction of ion current owing to positive sulfate peaks for each meteoritic particle, whereas Figure 6b shows the fraction due to the NO^+ peak. There is a clear enhancement of NO^+ in the ice residue when compared to the outside cloud particles, consistent with uptake of a gas-phase species such as HNO_3 (see text). There is no enhancement of sulfate as would be expected if ice crystals had scavenged sulfate-rich interstitial particles.

freezing occurs primarily by a homogeneous mechanism. The data acquired during CRYSTAL-FACE would suggest that both mechanisms, homogeneous freezing of sulfate and organic particles and sea salt and heterogeneous freezing of mineral dust and fly ash, can occur at the same geographic region at the same time of year. Furthermore, we observed a very high frequency of mineral dust in cirrus ice residue concurrent with a Saharan Dust transport event. This event fundamentally altered the chemical composition of the ice residue and most probably the mechanism by which freezing occurred. This result shows that the mechanism by which freezing occurs can be complexly linked to meteorology and episodic transport and should not be reduced to only a function of hemisphere and time of year.

[35] The overall abundance of mineral dust within cirrus ice during CRYSTAL-FACE was a result of transport throughout the mission from Africa. Mass spectra of mineral particles, in particular those acquired during the intense dust event, were observed to be composed almost exclusively of refractory components. This is significant in that recent laboratory studies have focused on the nucleation of ice from mineral dust encapsulated by thick layers of aqueous sulfate species [*Zuberi et al.*, 2002; *Hung et al.*, 2003]. These observations, of mineral dust that resided in the atmosphere for a week [*DeMott et al.*, 2003b] is significant because it implies that little soluble material, such as sulfate species, nitrates, or organics, was present on the particulate surface. Although PALMS is not quantitative, the lack of any sulfate signal for the mineral dust particles excludes the possibility of thick coatings. Laboratory studies of bare, or minimally coated, refractory surfaces would be of atmospheric relevance.

[36] The presence of significant amounts of mineral dust and sea salt near the tropopause in the form of cirrus ice residue, when almost none exist elsewhere in the UT/LS, implies a connection between the lowermost regions of the troposphere and anvil cirrus clouds. During the dust event, most ice residue at and above 12 km contained mineral dust

particles which formed a layer between 1 and 5 km [*Sassen et al.*, 2003; *DeMott et al.*, 2003b]. The mechanism by which freezing occurred, heterogeneous versus homogeneous as well as particle size, play a role in selection of particles which initiate ice formation [*Pruppacher and Klett*, 1978; *DeMott et al.*, 1997], but it is clear that an understanding of cloud structure and dynamics is critical for understanding tropical anvil cirrus clouds.

[37] *Koop et al.* [2000] have proposed a theory that described aerosol particle freezing as solely a function of water activity. This theory has been extended to simplify the modeling of atmospheric ice nucleation and cloud formation, typically by assuming a background population composed of sulfate aerosol particles [*Karcher and Lohmann*, 2002; *Karcher and Strom*, 2003]. During the southern flights and in the Florida area it was observed that interstitial aerosol did not have the same chemical composition as ice residue, although homogeneous freezing was the likely ice formation mechanism. Since all aerosol particles, those which froze or remained unfrozen, experienced the same relative humidity, this shows that the water activity of a sulfate-only population of aerosols is not sufficient to describe ice nucleation in the atmosphere. At a minimum, various aerosol particle compositions need to be taken into account. Although the theory espoused by *Koop et al.* [2000] is generally consistent with our observations of the preferential freezing of more active particles, such as large sea salt aerosol particles, it remains to be seen if the Koop et al. water activity model fully accounts for the diverse chemical nature of atmospheric particles.

Appendix A

[38] The counter flow virtual impactor used in these studies has not been subject to the detailed numerical modeling described in the work of *Laucks and Twohy* [1998]. Simple stopping distance calculations, described in the text and Figure 2, show that ice crystals from 5 to 22 micrometers in diameter were able to penetrate the counter flow but stop within the heated region of the CVI. We assumed crystals are spherical, in general agreement with images of cirrus ice of this size which suggest spheroids or droxtals [*Ohtake*, 1970]. It is also assumed that larger crystals are pumped away or impact the aft wall of the CVI because only particles smaller than $\sim$5 μm diameter are able to enter the PALMS sample flow 90° off the through flow path [*Okazaki et al.*, 1987; *Hangal and Willeke*, 1990]. The cutpoints are in agreement with more complicated calculations, described by *Laucks and Twohy* [1998] and *Pruppacher and Klett* [1978], which detail the process of evaporation on the basis of the actual particle residence time within the dry heated region of the CVI. It should be noted that evaporation occurs within a much shorter portion of the CVI than does stopping. This is because evaporation takes place after the velocity of incoming ice crystals have been reduced from aircraft to flow velocity. We therefore describe here ice residue from 0.12 to 2.0 micrometers diameter (the sensitivity limits of the PALMS instrument, see text for details) for ice crystals from 5 to 22 micrometers in diameter.

[39] The efficiency with which the CVI excluded interstitial aerosol was calculated by comparing the rate at which data were acquired with the counter flow on versus off while the WB-57F was outside of cloud, defined as the presence of less than 1 ice crystal detected per liter by the CAPS instrument [*Baumgardner et al.*, 2002]. The average PALMS acquisition rate in the UT/LS during cloud-free periods during CRYSTAL-FACE was 1.5 mass spectra per second with the counter flow off, 0.0003 Hz with the counter flow on, corresponding to a separation efficiency of 99.98%. This figure is a lower limit because some fraction of the mass spectra acquired with the counter flow on outside cloud may have been due to ice crystals which fell into the WB-57F flightpath from cirrus at higher altitudes or extremely large, but rare, background aerosol particles.

[40] The efficiency with which small ice crystal residue was analyzed when the counter flow was off within cirrus clouds is more difficult to quantify and assumptions are required. During these periods the goal was to sample only the interstitial aerosol by eliminating the counter flow and decreasing the particle residence time, from 0.4 to 0.09 s, in the heated section of the CVI by increasing the through flow rate (see Figure 2). Small ice crystals, those a few micrometers in diameter, would have entered, been heated, melted, and evaporated even within the relatively short residence time during these periods. Small crystal ice residue would then have been incorporated into the sample flow to PALMS. Measurement of the number density of small ice crystals is notoriously difficult and there exist large instrumental differences (D. Baumgardner, Universidad Nacional Autónoma de México, personal communication, 2003). We have therefore eliminated any interstitial data acquired when CAPS indicated ice crystal concentrations were greater than 100 crystals per liter. This would correspond to less than 0.2% of the average number of UT/LS aerosol particles measured during CRYSTAL-FACE from 90 to 1300 nanometer diameter by the FCAS instrument on the WB-57F [*Jonsson et al.*, 1995]. Enhancements, owing to nonisokinetic inlet effects between small ice crystals and unactivated aerosol particles, are on the order of 70 for PALMS at typical aircraft velocities. Under these conditions the maximum error in the interstitial aerosol owing to small ice crystals is <14%.

[41] **Acknowledgments.** This work was supported by NASA and NOAA base funding. The authors would like to thank Paul DeMott, Daryl Baumgardner, Paul Lawson, Jessica Smith, Ann Fridlind, and Chuck Wilson for useful discussions and data and the air and ground crews of the NASA WB-57F aircraft.

References

Abbatt, J. P. D. (2003), Interactions of atmospheric trace gases with ice surfaces: Adsorption and reaction, *Chem. Rev.*, *103*(12), doi:10.1021/cr0206418, 4783–4800.

Baumgardner, D., H. Jonsson, W. Dawson, D. O. Connor, and R. Newton (2002), The cloud, aerosol and precipitation spectrometer (CAPS): A new instrument for cloud investigation, *Atmos. Res.*, *59–60*, 251–264.

Bertram, A. K., T. Koop, L. T. Molina, and M. J. Molina (2000), Ice formation in $(NH_4)_2SO_4$-H_2O particles, *J. Phys. Chem. A*, *104*, 584–588.

Chen, Y., S. M. Kreidenweis, L. M. McInnes, D. C. Rogers, and P. J. DeMott (1998), Single particle analyses of ice nucleating aerosols in the upper troposphere and lower stratosphere, *Geophys. Res. Lett.*, *25*, 1391–1394.

Chen, Y., P. J. DeMott, S. M. Kreidenweis, D. C. Rogers, and D. E. Sherman (2000), Ice formation in sulfate and sulfuric acid aerosol particles under upper tropospheric conditions, *J. Atmos. Sci.*, *57*, 3752–3766.

Cziczo, D. J., and J. P. D. Abbatt (1999), Deliquescence, efflorescence and supercooling of ammonium sulfate aerosols at low temperature: Implica-

tions for cirrus cloud formation and aerosol phase in the atmosphere, *J. Geophys. Res.*, *104*, 13,781–13,790.
Cziczo, D. J., D. S. Thomson, and D. M. Murphy (2001), Ablation, flux, and atmospheric implications of meteors inferred from stratospheric aerosol, *Science*, *291*, 1772–1775.
DeMott, P. J., D. C. Rogers, and S. M. Kreidenweis (1997), The susceptibility of ice formation in upper tropospheric clouds to insoluble aerosol components, *J. Geophys. Res.*, *102*, 19,575–19,584.
DeMott, P. J., D. J. Cziczo, A. J. Prenni, D. M. Murphy, S. M. Kreidenweis, D. S. Thomson, and R. Borys (2003a), Measurements of the concentration and composition of nuclei for cirrus formation, *Proc. Natl. Acad. Sci.*, *100*(25), doi:10.1073/pnas.253267100, 14,655–14,660.
DeMott, P. J., K. Sassen, M. R. Poellot, D. Baumgardner, D. C. Rogers, S. D. Brooks, A. J. Prenni, and S. M. Kreidenweis (2003b), African dust aerosols as atmospheric ice nuclei, *Geophys. Res. Lett.*, *30*(14), 1732, doi:10.1029/2003GL017410.
Gard, E. E., et al. (1998), Direct observation of heterogeneous chemistry in the atmosphere, *Science*, *279*, 1184–1188.
Gross, D. S., M. E. Galli, P. J. Silva, and K. A. Prather (2000), Relative sensitivity factors for alkali metal and ammonium cations in single-particle aerosol time-of-flight mass spectra, *Anal. Chem.*, *72*, 416–422.
Hangal, S., and K. Willeke (1990), Overall efficiency of tubular inlets sampling at 0–90 degrees from horizontal aerosol flows, *Atmos. Environ. Part A*, *24*, 2379–2386.
Hartmann, D. L., M. E. Ockert-Bell, and M. L. Michelsen (1992), The effect of cloud type on Earth's energy balance: Global analysis, *J. Clim.*, *5*, 1281–1304.
Heintzenberg, J., K. Okada, and J. Strom (1996), On the composition of non-volatile material in upper tropospheric aerosols and cirrus crystals, *Atmos. Res.*, *41*, 81–88.
Heymsfield, A. J., and G. M. McFarquhar (1996), High albedos of cirrus in the tropical pacific warm pool: Microphysical interpretations from CEPEX and from Kwajalein, Marshall Islands, *J. Atmos. Sci.*, *53*, 2424–2451.
Heymsfield, A. J., and L. M. Miloshevich (1995), Relative humidity and temperature influences on cirrus formation and evolution: Observations from wave clouds and FIRE II, *J. Atmos. Sci.*, *52*, 4302–4326.
Hung, H.-M., A. Malinowski, and S. T. Martin (2003), Kinetics of heterogeneous ice nucleation on the surfaces of mineral dust cores inserted into aqueous ammonium sulfate particles, *J. Phys. Chem. A*, *107*, 1296–1306.
Intergovernmental Panel on Climate Change (2001), *Climate Change 2001, The Scientific Basis*, edited by J. T. Houghton et al., Cambridge Univ. Press, New York.
Jensen, E., W. G. Read, J. Mergenthaler, B. J. Sandor, L. Pfister, and A. Tabazadeh (1999), High humidities and subvisible cirrus near the tropical tropopause, *Geophys. Res. Lett.*, *26*, 2347–2350.
Jensen, E., D. O. C. Starr, and O. B. Toon (2004), CRYSTAL-FACE mission, *Eos Trans. AGU*, in press.
Jonsson, H. H., et al. (1995), Performance of a focused cavity aerosol spectrometer for measurements in the stratosphere of particle size in the 0.06–2.0 micrometer diameter range, *J. Ocean. Atmos. Technol.*, *12*, 115–129.
Karcher, B., and U. Lohmann (2002), A Parameterization of cirrus cloud formation: Homogeneous freezing including effects of aerosol size, *J. Geophys. Res.*, *107*(D23), 4698, doi:10.1029/2001JD001429.
Karcher, B., and J. Strom (2003), The roles of dynamical variability and aerosols in cirrus cloud formation, *Atmos. Chem. Phys. Discuss.*, *3*, 1415–1451.
Knollenberg, R. G., A. J. Dacher, and D. Huffman (1982), Measurements of the aerosol and ice crystal populations in tropical stratospheric cumulonimbus anvils, *Geophys. Res. Lett.*, *9*, 613–616.
Koop, T., B. Luo, A. Tsias, and T. Peter (2000), Water activity as the determinant for homogeneous ice nucleation in aqueous solutions, *Nature*, *406*, 611–614.
Laskin, A., M. J. Iedema, and J. P. Cowin (2002), Quantitative time-resolved monitoring of nitrate formation in sea salt particles using a CCSEM/EDX single particle analysis, *Environ. Sci. Technol.*, *36*, 4948–4955.
Laucks, M. L., and C. H. Twohy (1998), Size-dependent collection efficiency of an airborne counterflow virtual impactor, *Aero. Sci. Technol.*, *28*, 40–61.
Lin, R.-F., et al. (2002), Cirrus parcel model comparison project, phase 1: The critical components to simulate cirrus initiation explicitly, *J. Atmos. Sci.*, *59*, 2305–2329.
Liou, K.-N. (1986), Influence of cirrus clouds on weather and climate processes: A global perspective, *Mon., Weather Rev.*, *114*, 1167–1199.
Middlebrook, A. M., et al. (2003), A comparison of particle mass spectrometers during the 1999 Atlanta Supersite Project, *J. Geophys. Res.*, *108*(D7), 8424, doi:10.1029/2001JD000660.
Murphy, D. M., and D. S. Thomson (2000), Halogen ions and NO^+ in the mass spectra of aerosols in the upper troposphere and lower stratosphere, *Geophys. Res. Lett.*, *27*, 3217–3220.
Murphy, D. M., D. S. Thomson, and M. J. Mahoney (1998a), In situ measurements of organics, meteoritic material, mercury, and other elements in aerosols at 5 to 19 kilometers, *Science*, *282*, 1664–1669.
Murphy, D. M., D. S. Thomson, A. M. Middlebrook, and M. E. Schein (1998b), In situ single-particle characterization at Cape Grim, *J. Geophys. Res.*, *103*, 16,485–16,491.
Murphy, D. M., A. M. Middlebrook, and M. Warshawsky (2003), Cluster analysis of data from the Particle Analysis by Laser Mass Spectrometry (PALMS) instrument, *Aero. Sci. Techmol.*, *37*, 382–391.
Murphy, D. M., D. J. Cziczo, P. K. Hudson, M. E. Schein, and D. S. Thomson (2004), Particle density inferred from simultaneous optical and aerodynamic diameters sorted by composition, *J. Aerosol Sci.*, *35*, 135–139.
Ogren, J. A., J. Heintzenberg, and R. J. Charlson (1985), In situ sampling of clouds with a droplet to aerosol converter, *Geophys. Res. Lett.*, *12*, 121–124.
Ohtake, T. (1970), Unusual crystals in ice fog, *J. Atmos. Sci.*, *27*, 509–511.
Okazaki, K., R. W. Wiener, and K. Willeke (1987), The combined effect of aspiration and transmission on aerosol sampling accuracy for horizontal isoaxial sampling, *Atmos. Environ.*, *21*, 1181–1185.
Petzold, A., J. Strom, S. Ohlsson, and F. P. Schroder (1998), Elemental composition and morphology of ice-crystal residual particles in cirrus clouds and contrails, *Atmos. Res.*, *49*, 21–34.
Prenni, A. J., M. E. Wise, S. D. Brooks, and M. A. Tolbert (2001), Ice nucleation in sulfuric acid and ammonium sulfate particles, *J. Geophys. Res.*, *106*, 3037–3044.
Pruppacher, H. R., and J. D. Klett (1978), *Microphysics of Clouds and Precipitation*, D. Reidel, Norwell, Mass.
Sassen, K., P. J. DeMott, J. M. Prospero, and M. R. Poellot (2003), Saharan dust storms and indirect aerosol effects on clouds: CRYSTAL-FACE results, *Geophys. Res. Lett.*, *30*(12), 1633, doi:10.1029/2003GL017371.
Schreiner, J., C. Voigt, P. Zink, A. Kohlmann, D. Knopf, C. Weisser, P. Budz, and K. Mauersberger (2002), A mass spectrometer system for analysis of polar stratospheric aerosols, *Ref. Sci. Instrum.*, *73*, 446–452.
Seifert, M., J. Strom, R. Krejci, A. Minikin, A. Petzold, J.-F. Gayet, U. Schumann, and J. Ovarlez (2002), In situ observations of aerosol particles remaining from evaporated cirrus crystals: Comparing clean and polluted air masses, *Atmos. Chem. Phys. Discuss.*, *2*, 1599–1633.
Tabazadeh, A., Y. S. Djikaev, and H. Reiss (2002), Surface crystallization of supercooled water in clouds, *Proc. Natl. Acad. Sci.*, *99*, 15,873–15,878.
Thomson, D. S., A. M. Middlebrook, and D. M. Murphy (1997), Thresholds for laser-induced ion formation from aerosols in a vacuum using ultraviolet and vacuum-ultraviolet laser wavelengths, *Aero. Sci. Technol.*, *26*, 544–559.
Thomson, D. S., M. E. Schein, and D. M. Murphy (2000), Particle analysis by laser mass spectrometry WB-57F instrument overview, *Aero. Sci. Technol.*, *33*, 153–169.
Tuck, A. F., et al. (1997), The Brewer-Dobson circulation in the light of high altitude in situ aircraft observations, *Q. J. R. Meteorol. Soc.*, *123*, 1–63.
Twohy, C. H., and B. W. Gandrud (1998), Electron microscope analysis of residual particles from aircraft contrails, *Geophys. Res. Lett.*, *25*, 1359–1362.
Vohl, O., S. K. Mitra, K. Diehl, G. Huber, S. C. Wurzler, K.-L. Kratz, and H. R. Pruppacher (2001), A wind tunnel study of turbulence effects on the scavenging of aerosol particles by water drops, *J. Atmos. Sci.*, *58*, 3064–3072.
Willeke, K., and P. A. Baron (Eds.) (1992), *Aerosol Measurement*, Van Nostrand Reinhold, New York.
Wilson, J. C., and B. Y. H. Liu (1980), Aerodynamic particle size measurement by laser-Doppler velocimetry, *J. Aerosol Sci.*, *11*, 139–150.
Wise, M. E., S. D. Brooks, R. M. Garland, D. J. Cziczo, S. T. Martin, and M. A. Tolbert (2003), Solubility and freezing effects of Fe^{2+} and Mg^{2+} in H_2SO_4 solutions representative of upper tropospheric and lower stratospheric sulfate particles, *J. Geophys. Res.*, *108*(D14), 4434, doi:10.1029/2003JD003420.
Zuberi, B., A. K. Bertram, C. A. Cassa, L. T. Molina, and M. J. Molina (2002), Heterogeneous nucleation of ice in $(NH_4)_2SO_4$-H_2O particles with mineral dust immersions, *Geophys. Res. Lett.*, *29*(10), 1504, doi:10.1029/2001GL014289.

D. J. Cziczo, P. K. Hudson, D. M. Murphy, and D. S. Thomson, Aeronomy Laboratory, National Oceanic and Atmospheric Administration, 325 Broadway, R/AL6, Boulder, CO 80305, USA. (djcziczo@al.noaa.gov; phudson@al.noaa.gov; dmurphy@al.noaa.gov; dthomson@al.noaa.gov)